

Compact Intracloud Discharges

Los Alamos
NATIONAL LABORATORY

*Los Alamos National Laboratory is operated by the University of California
for the United States Department of Energy under contract W-7405-ENG-36.*

This work was supported by the US Department of Energy, NN-20.

This thesis was accepted by the Department of Electrical Engineering, University of Colorado, Boulder, Colorado, in partial fulfillment of the requirements for the degree of Doctor of Philosophy. The text and illustrations are the independent work of the author and only the front matter has been edited by the CIC-1 Writing and Editing Staff to conform with Department of Energy and Los Alamos National Laboratory publication policies.

An Affirmative Action/Equal Opportunity Employer

This report was prepared as an account of work sponsored by an agency of the United States Government. Neither The Regents of the University of California, the United States Government nor any agency thereof, nor any of their employees, makes any warranty, express or implied, or assumes any legal liability or responsibility for the accuracy, completeness, or usefulness of any information, apparatus, product, or process disclosed, or represents that its use would not infringe privately owned rights. Reference herein to any specific commercial product, process, or service by trade name, trademark, manufacturer, or otherwise, does not necessarily constitute or imply its endorsement, recommendation, or favoring by The Regents of the University of California, the United States Government, or any agency thereof. The views and opinions of authors expressed herein do not necessarily state or reflect those of The Regents of the University of California, the United States Government, or any agency thereof. Los Alamos National Laboratory strongly supports academic freedom and a researcher's right to publish; as an institution, however, the Laboratory does not endorse the viewpoint of a publication or guarantee its technical correctness.

Compact Intracloud Discharges

David A. Smith

ACKNOWLEDGMENTS

I would like to take this opportunity to express my gratitude to the members of my dissertation committee, to my colleagues at Los Alamos National Laboratory (LANL) and the New Mexico Institute of Mining and Technology (NMIMT), to LANL and the Department of Energy for funding this research, and to my friends and family who have provided advice, support, and assistance to me since I began my graduate work five years ago.

Dan Holden, a Los Alamos technical staff member and a member of my committee, has been my mentor at Los Alamos for nine years. As well as being a good friend with whom I have shared countless adventures, Dan has been a tremendous positive influence on me and has provided me with numerous opportunities to learn and grow both personally and professionally. Thank you, Dan.

I would also like to express my gratitude to the other members of my University of Colorado (CU) graduate committee: Susan Avery, my advisor, Electrical Engineering faculty member, and Director of the Cooperative Institute for Research in Environmental Sciences; Jeffrey Forbes, Aerospace Engineering faculty member; Melinda Piket-May, Electrical Engineering faculty member, and Robert Serafin, Director of the National Center for Atmospheric Research. These people were very supportive of my cooperative research effort between the Department of Electrical

Engineering at CU and the Space and Atmospheric Science group at Los Alamos, and provided valuable constructive feedback during our many sessions together.

Numerous workers at Los Alamos deserve recognition for their contributions to this research. The following present and former technical staff members of the Radio and Ionospheric Physics team took the time to share with me their expertise in disciplines ranging from thunderstorm electrification to ionospheric propagation: Paul Argo, Joe Fitzgerald, Abe Jacobson, Bob Massey, Charley Rhodes, Bob Roussel-Dupré, and Xuan-Min Shao. In addition to thanking these people, I would also like to express my gratitude to Marx Brook and Paul Krehbiel of NMIMT, who both made significant contributions to my understanding of the physical processes that occur during thunderstorms. Countless Los Alamos personnel not already mentioned provided generously of their time and/or resources in assisting me with various aspects of the research detailed in this dissertation. These people include Dot DeLapp, Jim Devenport, Mary Dugan, Bob Franz, Dave Guenther, Phil Klingner, Eloisa Michel, Karen Olivas, Marty Shipley, Gary Stelzer, Brian Wiemers, and Hong-Hong Zhu. I sincerely appreciate the assistance provided by these people. Bob Franz and Xuan-Min Shao deserve special mention for providing me with computer programs that they authored and that allowed me to complete portions of my analyses. I would also like to single out two people who were not on my committee, but who provided generously of their time to proofread entire drafts of my dissertation and provide me with valuable feedback: Bob Massey and my mom.

Funding for this research was provided by the Department of Energy. I gratefully acknowledge their support and the enthusiastic support provided by Los Alamos National Laboratory and the Space and Atmospheric Science group, NIS-1.

Finally I would like to thank my friends and family for their loyal support, especially during these past four months as I chose to curtail many of my regular social and recreational activities in order to focus on the completion of my dissertation. My mom, dad, brother Leo, and best friend Shayna deserve special recognition here. Thank you to all of you.

CONTENTS

CHAPTER		PAGE
1	INTRODUCTION	1
1.1	BLACKBEARD AND TRANSIONOSPHERIC PULSE PAIRS (TIPPs)	2
1.1.1	One-Source Hypothesis	8
1.1.2	Two-Source Hypothesis	17
1.2	SUBIONOSPHERIC PULSE PAIRS (SIPPs)	19
1.2.1	Dispersed Subionospheric Pulse Pairs	20
1.2.2	Undispersed Subionospheric Pulse Pairs	23
1.3	NARROW POSITIVE BIPOLAR PULSES (NPBPs)	25
1.4	COMPACT INTRACLOUD DISCHARGES (CIDs)	30
2	INSTRUMENTATION	32
2.1	ELECTRIC FIELD CHANGE INSTRUMENTATION	33
2.1.1	Field Change Meters	35
2.1.2	Field Change Meter Calibration	42
2.2	BROADBAND HF INSTRUMENTATION	45
2.2.1	Broadband HF Receivers	46

2.2.2	Broadband HF System Calibration	50
2.3	BLACKBEARD	57
2.3.1	Blackbeard Timing Calibration	61
3	SOURCE LOCATION METHODOLOGY	66
3.1	SOURCE LOCATIONS FROM GROUND-BASED MEASUREMENTS	72
3.1.1	Location Method One: Three or More TOA Receivers	74
3.1.2	Location Method Two: Two TOA Receivers	80
3.1.3	Other Location Notes	84
3.2	SOURCE LOCATIONS FROM GROUND- AND SATELLITE-BASED MEASUREMENTS	85
4	OBSERVATIONS FROM THREE SOUTHWESTERN THUNDERSTORMS ...	86
4.1	ELECTRIC FIELD CHANGE AND HF WAVEFORMS FROM CIDS	87
4.2	WAVEFORMS FROM CLOUD-TO-GROUND, AND INTRACLOUD LIGHTNING	98
4.3	CID LOCATIONS	101
4.3.1	Storm 1	103
4.3.2	Storm 2	105
4.3.3	Storm 3	108
4.3.4	Observations from all Three Storms	111
4.4	CID TEMPORAL CONTEXT	117

4.5	RADAR REFLECTIVITY OBSERVATIONS	121
4.5.1	Storm 3	121
4.5.2	Storm 1	127
5	OBSERVATIONS FROM TROPICAL CYCLONE FAUSTO	132
5.1	FIRST COINCIDENT EVENT: 11 SEPTEMBER 1996	135
5.1.1	Temporal Context of the Events Recorded on 11 September	140
5.1.2	HF Propagation Model	147
5.1.3	Location Technique One: Source Height and Pulse Separations	155
5.1.4	Location Technique Two: Source Range and DTOA	158
5.1.5	Data from the National Lightning Detection Network	162
5.1.6	A Comparison of the Location Techniques	167
5.1.7	GOES-8 Infrared Imagery	171
5.2	SECOND COINCIDENT EVENT: 19 SEPTEMBER 1996	171
5.3	OVERVIEW OF COINCIDENT GROUND AND SATELLITE OBSERVATIONS	188
6	CID WAVEFORMS AND PHENOMENOLOGY	193
6.1	CID ELECTRIC FIELD CHANGE EMISSIONS	193
6.1.1	NPBP Temporal Isolation	196

6.1.2	NPBP Amplitude	201
6.1.3	NPBP Duration and Risettime	209
6.2	CID HF AND VHF RADIO EMISSIONS	211
6.2.1	CID RF Temporal Isolation	212
6.2.2	CID RF Duration	215
6.2.3	CID RF Amplitude/Power	216
6.3	SOURCE REGION PHENOMENOLOGY	218
7	CID PHYSICAL CHARACTERISTICS	225
7.1	SOURCE ORIENTATION AND RADIATION PATTERN	225
7.2	CID SIZE, CHARGE, AND CURRENT	228
7.3	ELECTRIC FIELDS AND CHARGE DENSITIES PRIOR TO CIDs	239
8	CONCLUSION	245
	GLOSSARY OF TERMS AND ACRONYMS	253
	REFERENCES	257

TABLES

NUMBER		PAGE
	2. Instrumentation	
2.1	Electric field change meter characteristics	41
	4. Observations from Three Southwestern Thunderstorms	
4.1	Source and ionosphere height calculations	115
	5. Observations from Tropical Cyclone Fausto	
5.1	HF propagation model inputs and outputs	154
	6. CID Waveforms and Phenomenology	
6.1	Mean NPBP characteristics	195
6.2	Comparison of NPBP initial and overshoot peak	
	Amplitudes	202
6.3	Results from VLF/LF propagation model	206
6.4	Comparison of amplitudes of NPBPs and IC/CG	
	waveforms	207

6.5	NPBP FWHMs, durations, and risetimes	210
6.6	Mean CID RF characteristics	212
6.7	Temporal isolation of RF radiation from CIDs	213
6.8	Comparison of RF from CIDs and IC/CG lightning flashes	218

7. CID Physical Characteristics

7.1	Computed physical characteristics of CIDs	232
7.2	Comparison of CIDs to other lightning processes	237

FIGURES

NUMBER		PAGE
1. Introduction		
1.1	Spectrogram of TIPP event	6
1.2	One-source versus two-source hypotheses	9
1.3	Illustration of source/receiver geometry	11
1.4	Pulse time separation as a function of elevation angle	12
1.5	TIPP separation histogram	14
1.6	Dispersed SIPP	21
1.7	Dispersed lightning	22
1.8	Undispersed SIPP	24
1.9	NPBP from Le Vine [1980]	27
1.10	NPBP from Willett et al. [1989]	29
2. Instrumentation		
2.1	Map showing locations of recording stations and storms ...	34
2.2	Photograph of electric field change meter	36
2.3	Schematic diagram of electric field change meter circuit ...	38

2.4	Block diagram of LANL electric field change meter	40
2.5	Illustration of calibration electric field change meter	43
2.6	Block diagram of LANL broadband HF system	47
2.7	Photograph of HF discone antenna	48
2.8	Computer wire-frame model of discone antenna	51
2.9	Beam pattern of discone antenna from computer model	53
2.10	VSWR of discone antenna	54
2.11	HF system transmission loss	56
2.12	Photograph of ALEXIS satellite	58
2.13	Block diagram of Blackbeard	59
2.14	Photograph of the Los Alamos Portable Pulser	62
2.15	Spectrogram of LAPP shot	64
2.16	Histogram of Blackbeard timing differences	65
3. Source Location Methodology		
3.1	Illustration of DTOA isochrones	68
3.2	Diagram of propagation paths and image receivers	70
3.3	Diagram for 3-station 2-D location method	76
3.4	Diagram for 2-station 3-D location method	83
4. Observations from Three Southwestern Thunderstorms		
4.1	CID from storm 3 (#1)	88

4.2	CID from storm 3 (#2)	90
4.3	Multiple-hop NPBP from storm over Mexico	92
4.4	CID from storm 1	95
4.5	HF reflection geometry for three storms	96
4.6	CID from storm 2	97
4.7	Cloud-to-ground lightning stroke	100
4.8	Intracloud lightning stroke	102
4.9	Storm 1 plan view source locations	104
4.10	Storm 1 source heights	106
4.11	Storm 2 plan view source locations	107
4.12	Storm 2 source heights	109
4.13	Storm 3 plan view source locations	110
4.14	Storm 3 source heights	112
4.15	All storm source heights	114
4.16	All storm virtual ionosphere heights	116
4.17	Storm time histories	119
4.18	Radar reflectivity image: storm 3, 3.4°	122
4.19	Radar reflectivity image: storm 3, 4.3°	125
4.20	Radar reflectivity image: storm 3, 6.0°	126
4.21	Radar reflectivity image: storm 1, 0.5°	128
4.22	Radar reflectivity image: storm 1, 1.5°	129
4.23	Radar reflectivity image: storm 1, 2.4°	130

5. Observations from Tropical Cyclone Fausto

5.1	Coincident TIPP 11 September	136
5.2	Coincident CID 11 September	137
5.3	Whitened coincident CID 11 September	139
5.4	First TIPP 11 September	141
5.5	Second TIPP 11 September	142
5.6	Sub-satellite points and fields of view 11 September	144
5.7	Earlier CID 11 September	145
5.8	Whitened earlier CID 11 September	146
5.9	Time line for 11 September event detections	148
5.10	HF propagation paths	151
5.11	Source location method 1, 11 September	157
5.12	Source location method 1, zoom, 11 September	159
5.13	Source location method 2, 11 September	161
5.14	Source location methods 1 and 2, 11 September	163
5.15	NLDN data, 11 September	164
5.16	All location methods, 11 September	168
5.17	GOES-8 IR image from 11 September	172
5.18	Coincident TIPP 19 September	174
5.19	Second TIPP 19 September	175
5.20	Sub-satellite points and fields of view 19 September	176
5.21	Coincident CID 19 September	177

5.22	Whitened coincident CID 19 September	178
5.23	Later CID 19 September	179
5.24	Whitened later CID 19 September	180
5.25	Time line for 19 September event detections	181
5.26	Source location method 1, 19 September	184
5.27	Source location method 1, Zoom, 19 September	185
5.28	Source location method 2, 19 September	186
5.29	Source location methods 1 and 2, 19 September	187
5.30	All location methods, 19 September	189
5.31	GOES-8 IR image from 19 September	190

6. CID Waveforms and Phenomenology

6.1	Close-up views of NPBP from storm 3	197
6.2	NPBP followed by IC lightning activity	199
6.3	Response of propagation filter	204
6.4	Effect of propagation filter on synthesized NPBP	205
6.5	Discharge initiation altitudes from Proctor [1991]	221

7. CID Physical Characteristics

7.1	Time relationship between NPBP and RF radiation	230
7.2	Physical characteristics as a function of streamer velocity	240

7.3	Charge configuration for discharge model	241
7.4	Scatter plot of average current versus spatial extent	244

COMPACT INTRACLOUD DISCHARGES

David A. Smith

ABSTRACT

In November of 1993, mysterious signals recorded by a satellite-borne broadband VHF radio science experiment called Blackbeard led to a completely unexpected discovery. Prior to launch of the ALEXIS satellite, it was thought that its secondary payload, Blackbeard, would most often detect the radio emissions from lightning when its receiver was not overwhelmed by noise from narrowband communication carriers. Instead, the vast majority of events that triggered the instrument were isolated pairs of pulses that were one hundred times more energetic than normal thunderstorm electrical emissions. The events, which came to be known as TIPP's (for transionospheric pulse pairs), presented a true mystery to the geophysics community. At the time, it was not even known whether the events had natural or anthropogenic origins. After two and one half years of research into the unique signals, two ground-based receiver arrays in New Mexico first began to detect and record thunderstorm radio emissions that were consistent with the Blackbeard observations. On two occasions, the ground-based systems and Blackbeard even recorded emissions that were produced by the same exact events. From the ground-

based observations, it has been determined that TIPP events are produced by brief, singular, isolated, intracloud electrical discharges that occur in intense regions of thunderstorms. These discharges have been dubbed CIDs, an acronym for compact intracloud discharges. During the summer of 1996, ground-based receiver arrays were used to record the electric field change signals and broadband HF emissions from hundreds of CIDs. Event timing that was accurate to within a few microseconds made possible the determination of source locations using methods of differential time of arrival. Ionospheric reflections of signals were recorded in addition to groundwave/line-of-sight signals and were used to determine accurate altitudes for the discharges. Twenty-four CIDs were recorded from three thunderstorms in the southwestern United States (US). The events occurred at altitudes between 8 and 11 km above mean sea level (MSL). Radar reflectivity data from two of the storms showed that CIDs occurred in close spatial proximity to thunderstorm cores with peak radar reflectivities of 47 to 58 dBZ. Over one hundred CIDs were also recorded from tropical cyclone Fausto off the coast of Mexico. These events occurred at altitudes between 15 and 17 km MSL. CIDs are singular discharges that usually occur in temporal isolation from other thunderstorm radio emissions on time scales of at least a few milliseconds. Calculations show that the discharges are vertically oriented and 300 to 1000 m in spatial extent. They produce average currents of several tens to a couple hundred kA for time periods of approximately 15 μ s. Based on the results of a charge distribution model, the events occur in thunderstorm regions with charge densities on the order of several tens of nC/m³ and peak electric fields that are greater than 1×10^6 V/m. Both of these values are an order of magnitude greater than values

previously measured or inferred from *in situ* thunderstorm measurements. The unique radio emissions from CIDs, in combination with their unprecedented physical characteristics, clearly distinguish the events from other types of previously observed thunderstorm electrical processes.

CHAPTER 1

INTRODUCTION

A small (113 kg) satellite named ALEXIS (Array of Low Energy X-ray Imaging Sensors) was launched on a Pegasus booster on 25 April 1993 into a 750×850 km, 70° inclination orbit. ALEXIS was conceived of and built by Los Alamos National Laboratory (LANL) and carries two scientific payloads designed to test space-based technologies for detecting emissions from nuclear detonations (NUDETs). The primary payload, which carries the same name as the satellite, includes an array of six telescopes that collect ultrasoft X-ray emissions. The secondary payload, named Blackbeard, is a broadband VHF radio science experiment. Both payloads have made significant contributions to their programmatic missions and, in the process, have served as excellent platforms for unique astronomical and geophysical remote sensing research. ALEXIS has provided the first maps of celestial soft X-ray emissions. Blackbeard, from its perspective in low-earth orbit, discovered an entirely new and mysterious class of radio emissions from the earth. The distinct, paired emissions were dubbed transionospheric pulse pairs (TIPPs) by *Holden et al.* [1995], and have led to the identification of a unique type of thunderstorm electrical discharge. The discharges, which shall be referred to as compact intracloud discharges (CIDs), are compact intracloud lightning events that occur in the most intense regions of

thunderstorms. CIDs are distinct in many respects from other types of previously described thunderstorm electrical processes. These unique discharges are the subject of this dissertation.

1.1 BLACKBEARD AND TRANSIONOSPHERIC PULSE PAIRS (TIPPs)

Difficulties were encountered during the launch of the ALEXIS satellite. Premature deployment of a solar panel caused damage to its magnetometer and prevented ground controllers from making contact with the satellite until late June of 1993, two months after its launch into low-earth orbit. Modified attitude control procedures were implemented to minimize problems associated with the launch anomaly and full satellite operations were begun in late July. Details regarding the satellite, payloads, and subsequent operations have been described by *Priedhorsky et al.* [1993] and *Roussel-Dupré et al.* [1997].

The Blackbeard instrument was designed to test technologies related to the space-based detection and timing of electromagnetic pulses (EMPs) produced by nuclear weapons. The EMP from a nuclear explosion is a time-varying electromagnetic field that very rapidly (on the order of 10 nanoseconds) reaches its peak value and decays less quickly (during a few tens of microseconds) back to a negligible value. It is produced by asymmetries in the blast environment of a weapon that cause net time-varying currents to flow. Asymmetries may result from weapon design, proximity of the blast to the earth's surface, atmospheric air density gradients, or other

environmental constraints. A description of the EMP and its effects was published by *Glasstone and Dolan* [1977]. The EMP is notorious for its ability to damage unprotected electronic devices. It also provides a means of detecting and accurately locating NUDETs. Such a capability is a valuable asset for the worldwide monitoring of nuclear activities and for verifying international compliance with treaties of nonproliferation.

EMPs are powerful radio emissions that radiate across a broad spectrum of frequencies from tens of kHz or lower to at least several hundred MHz (as indicated approximately by the inverse of the EMP rise time). For this reason Blackbeard was designed as a broadband receiver, providing in a sense, a receiver matched to the emission source it was designed to detect. Blackbeard operates in the VHF portion of the electromagnetic spectrum because lower frequency radio emissions (HF and below) often do not escape the refractive effects of the earth's ionosphere and thus, do not reach low-earth orbit. EMP radio emission frequencies greater than VHF are less powerful, so, more difficult to detect. The matter of detecting and time tagging broadband VHF signals from orbit is complicated by the dispersive and refractive effects of the ionosphere. These effects become increasingly severe at lower frequencies in proportion to wavelength squared.

The Blackbeard radio receiver records waveforms using a fixed-rate 150 Msample/s, 8-bit digitizer that takes its input from either of a pair of wideband sub-resonant monopole antennas and a single-conversion VHF receiver. There are two bands from which the instrument can sample: a low band from 28 to 95 MHz and a high band from 108 to 166 MHz. Sixteen highpass and lowpass analog filters permit

further subdivision of either band. The instrument utilizes a level trigger to detect transient events. Details concerning the Blackbeard instrument and subsequent data acquisition were described by *Holden et al.* [1995] and *Massey and Holden* [1995].

Prior to the launch of Blackbeard it was known that radio emissions from natural lightning produced transient broadband emissions in the VHF spectrum and would be a potential source of false alarms for any system designed to detect a nuclear EMP. In fact much of the motivation for orbiting the Blackbeard payload was provided by the need to characterize the earth's radio background. The characterization was necessary for both transient signals, like those produced by lightning, and CW (continuous wave) signals, like those emitted by commercial radio and television stations.

Although Blackbeard provides a receiver well-matched to the detection of broadband transients, CW signals can still degrade its sensitivity when many, powerful carriers exist within its bandwidth. The detectability of transient signals in carrier-dominated radio environments was discussed by *Smith* [1995].

In November of 1993 the first Blackbeard geophysical study was begun. The goal of the study was to detect thunderstorm radio emissions over the equatorial inter-tropical convergence zone (ITCZ). Three months later, after determining optimal instrument gains, filter settings, and trigger thresholds, 85 events of subionospheric origin had been recorded. Two very remarkable and unexpected qualities characterized all of these events: 1. Every Blackbeard record contained exactly two transient signals that were separated by between 10 and 110 μ s; 2. The RF power in the paired signals was on the order of a hundred times greater than that from lightning emissions described by previous researchers. The mysterious, paired VHF pulses

were dubbed TIPP events by *Holden et al.* [1995]. To date, over 1100 of the events have been recorded by Blackbeard (Dorothea DeLapp, private communication).

An example of a TIPP electric field waveform from Blackbeard is shown in the upper panel of Figure 1.1. A time-frequency spectrogram of the waveform appears in the lower panel. The spectrogram shows the power in the signal as a function of frequency and time. It was formed by dividing the time series into a number of short, overlapping time series that were processed using the fast Fourier transform to determine short term power spectra. The resulting spectra were aligned vertically and a color scale was utilized to represent localized waveform log power. The spectrogram in Figure 1.1 was formed using a 128 point (850 ns) sliding Blackman window. Successive waveform segments were overlapped by 50%. The TIPP event in the spectrogram is the pair of powerful, dispersed transients. The VHF pulses are separated in time by approximately 60 μ s. Dispersion of the signals was caused by propagation through the ionosphere. The dim, horizontal lines in the figure are narrowband carrier signals, most likely from ground-based transmitters (ALEXIS was over central Africa when it recorded the event). The vertical lines that are most clearly visible at lower frequencies (below 35 MHz) were probably produced by the satellite itself, as suggested by their lack of dispersion and their frequent appearance in Blackbeard records.

Based on Blackbeard observations, TIPP events have the following general characteristics: By definition they are paired. Triggered records that contain pairs have greatly outnumbered (by a ratio greater than 10:1 as estimated by the this author) records that contain singular pulses or pulses with multiplicity greater than two. As

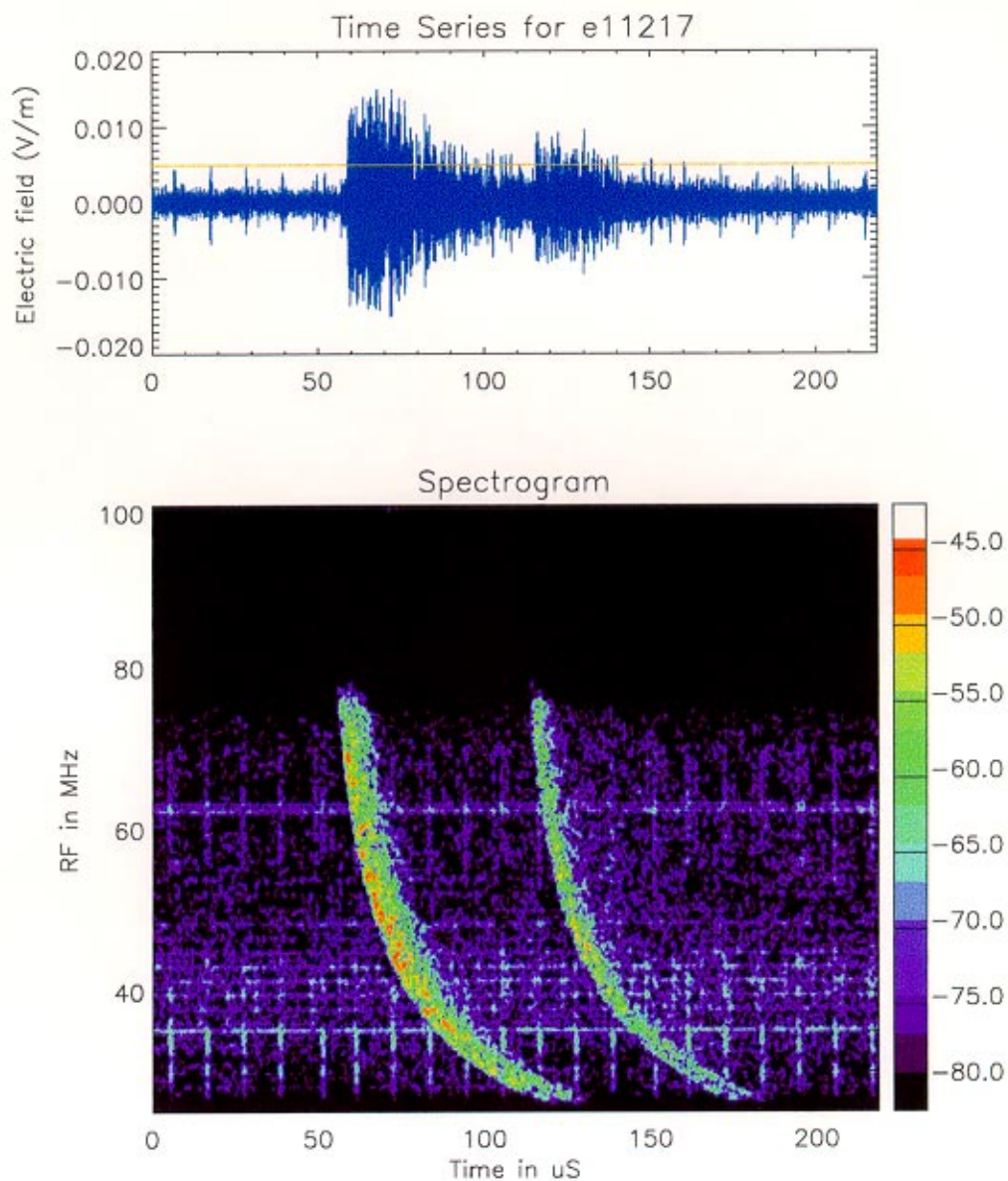


Figure 1.1: Electric field waveform and spectrogram of a transionospheric pulse pair (TIPP) event that was recorded by the Blackbeard instrument over Africa. The spectrogram color scale represents waveform power in dB as a function of time and frequency.

reported by *Massey and Holden* [1995], the mean duration for each pulse is 5 μs and the median duration is 3.8 μs (after the dispersive effects of the ionosphere have been removed by signal processing). Observed pulse separations have ranged from a few microseconds to greater than 100 μs , with the mean and median separations both being very close to 50 μs [*Massey and Holden*, 1995]. The low end of this distribution is difficult to characterize and interpret accurately because the two pulses become indistinguishable at a minimum separation that is on the order of the duration of each pulse. TIPP's radiate very strongly across the entire recording range of Blackbeard from 28 to 166 MHz. TIPP peak electric field values are about ten times greater than lightning peak electric fields that have been observed during ground-based studies of lightning radio emissions [*Holden et al.*, 1995]. It has been observed that TIPP events are most often recorded over locations and at times of day where and when thunderstorm activity is known to be most active [*Holden et al.*, 1995; *Zuelsdorf et al.*, 1997].

The most striking characteristic of TIPP recordings has been the fact that dual pulses have been recorded so much more frequently than pulses of other multiplicity. There is scant specific mention of double pulses in the literature describing previous observations of radio emissions from lightning. The observed time separations between the pulses (10 to 110 μs as reported by *Holden et al.* [1995]) are not inconsistent with previous reports of the inter-pulse spacing between RF (radio frequency) pulses during lightning flashes, but “normal” discharges most often consist of thousands to tens of thousands of pulses that are radiated during a flash that lasts a

few to many tenths of a second [Oetzel and Pierce, 1969, a; Proctor, 1973; Pierce, 1977]. The corresponding inter-pulse intervals are on the order of tens to hundreds of microseconds, but reports of pulses occurring with a multiplicity of exactly two have been scarce. Two hypotheses were proposed to explain why, in the overwhelming majority of Blackbeard recordings, paired pulses were received. The explanations, which shall be referred to as the one-source and two-source hypotheses, were introduced by *Holden et al.* [1995] and elaborated upon by *Massey and Holden* [1995], *Smith* [1995], *Smith and Holden* [1996], and *Massey et al.* [1998]. The one-source hypothesis considers the source of a TIPP to be a singular discharge that reflects with little loss from the surface of the earth. The reflection is recorded by Blackbeard as the second pulse. The two-source hypothesis considers a TIPP to result from two coupled discharges that occur at different times and/or in different locations. Figure 1.2 provides illustrations of the two hypotheses.

1.1.1 One-Source Hypothesis

Under the one-source hypothesis, the second pulse of a TIPP is the reflection of downward-directed source emissions from the surface of the earth. This possibility is illustrated in the upper panel of Figure 1.2. The measured time separation between the direct pulse and its reflection is a function of the height of the source above ground level and the position of the receiver with respect to the source. An approximate relationship between pulse time separation (Δt), source height (h), and satellite elevation angle (θ) is given by Equation 1.1:

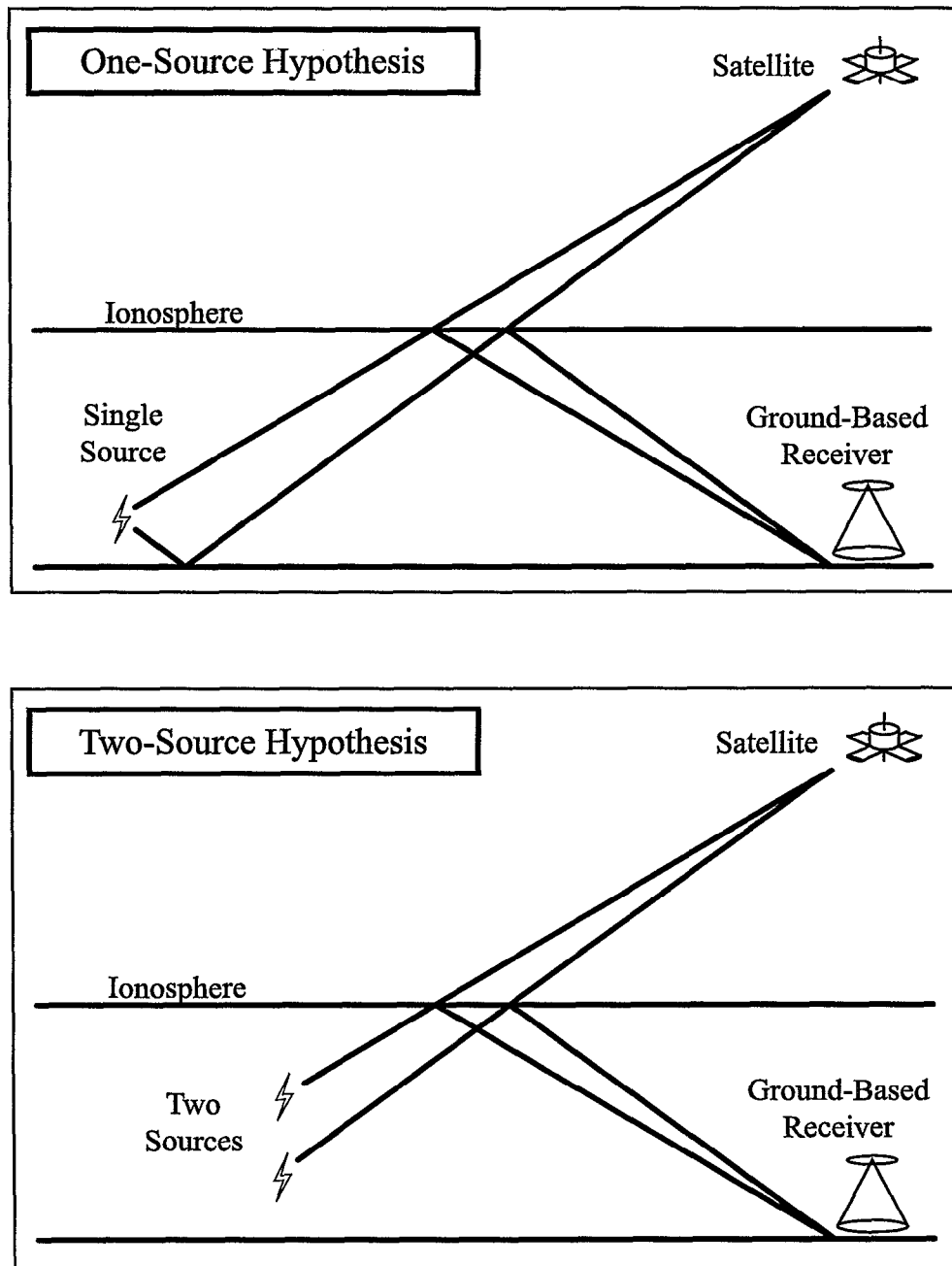


Figure 1.2: Illustrations of the one-source and two-source hypotheses for the production of TIPP (transionospheric pulse pair) and SIPP (subionospheric pulse pair) events.

$$\Delta t = \frac{2h \sin(\theta)}{c} \quad (1.1)$$

where c is the speed of light. This equation is approximately true for cases when the satellite altitude (H) is much greater than the source altitude (i.e. $H \gg h$).

Figure 1.3 illustrates the source and satellite geometry for the case described by Equation 1.1. Figure 1.4 shows the actual relationship between elevation angle and pulse separation for a source at a given height. The top graph shows pulse separation as a function of elevation angle for a source at an altitude of 10 km above ground level (AGL). From zenith, the satellite measures a separation of 67 μ s. From the limb ($\theta = 0^\circ$), the pulses are indistinguishable ($\Delta t = 0 \mu$ s). The bottom graph shows pulse separation normalized to the height of the source above ground (h). Note that at zenith ($\theta = 90^\circ$), the observed normalized pulse separation is 2.0. This means that the delay from the time of arrival (TOA) of the direct pulse to the TOA of the reflected pulse is equal to exactly two times the source height divided by the propagation velocity. This makes sense, because for the reflected pulse to be received, it must propagate straight down and back through the source origin, traveling an additional path length $2h$ compared to the direct pulse.

Equation 1.1 and Figures 1.3 and 1.4 show that the maximal time separation between pulses for a given source height occurs when the satellite is positioned directly above the source. Short time separations can occur from sources that are located near ground level (small h) or sources that occur near the horizon (small θ) as viewed from the satellite receiver.

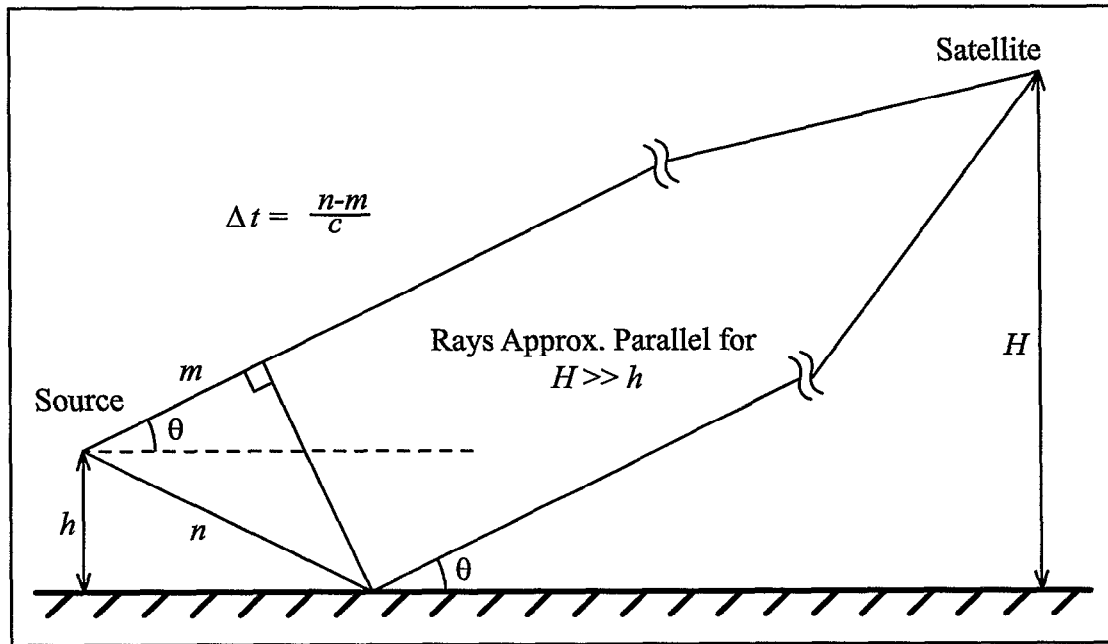


Figure 1.3: Illustration of the reflection geometry for the one-source hypothesis. The direct and reflected rays can be assumed to be parallel for $H \gg h$, under which condition the pulse time separation (Δt) is a function of the source height (h) and satellite elevation angle (θ) only.

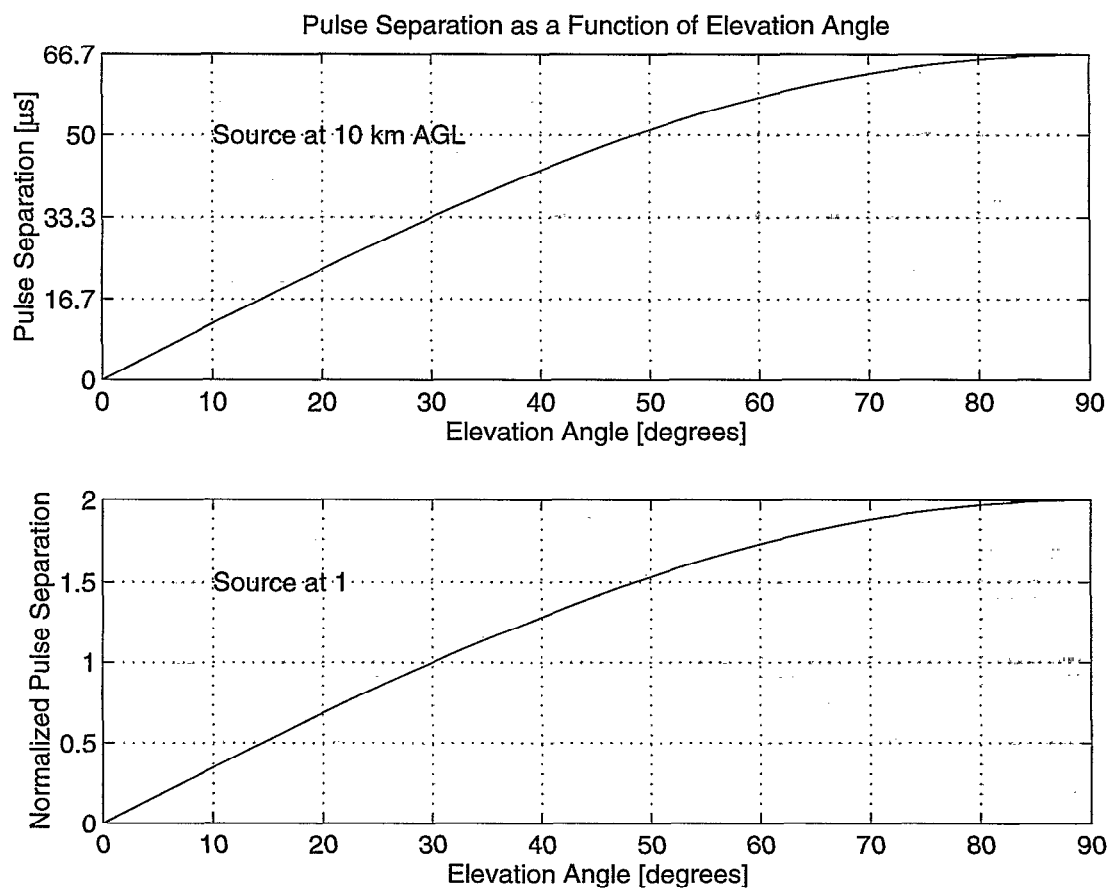


Figure 1.4: Plots of pulse separation as a function of elevation angle for sources at a fixed height. In the upper panel, the source height is 10 km above ground level (AGL) and pulse separation is given in microseconds. In the lower panel, pulse separation is normalized to a source height of 1 (arbitrary units).

The actual distribution of pulse separations for the first 84 TIPP events recorded by Blackbeard is shown in Figure 1.5 (adapted from *Massey and Holden* [1995]). Note that four events with time separations of less than 10 μs were received. Under the one source hypothesis, these events either occurred close to the earth's surface or were viewed from a shallow viewing angle by Blackbeard (or both).

At the far right end of the distribution in Figure 1.5 are TIPP events that had pulse separations as large as 100 μs . These events place a lower bound on the upper limit of source heights. That is, for a given measured pulse pair separation, the actual event source height must have been at least that which results from inverting Equation 1.1 and solving for h when the source is assumed to have occurred with the satellite at zenith ($\theta = 90^\circ$). For example, the largest pulse separation for a TIPP event recorded by Blackbeard has been approximately 120 μs (the event occurred after the distribution depicted in Figure 1.5 was formed). Under the one-source hypothesis, the height of the source would have had to have been at least 18 km above ground level, the value for h calculated from Equation 1.1 for $\theta = 90^\circ$ and $\Delta t = 120 \mu\text{s}$. The further from Blackbeard's nadir that source actually occurred, the higher in altitude the source would have had to have been in order to produce the measured time separation. Thus large time separations place a lower bound on the upper limit of the actual source height distribution. If the one-source hypothesis is correct, then the mechanism for the production of the singular discharge must allow for the possibility that the events can occur up to an altitude of at least 18 km above ground level.

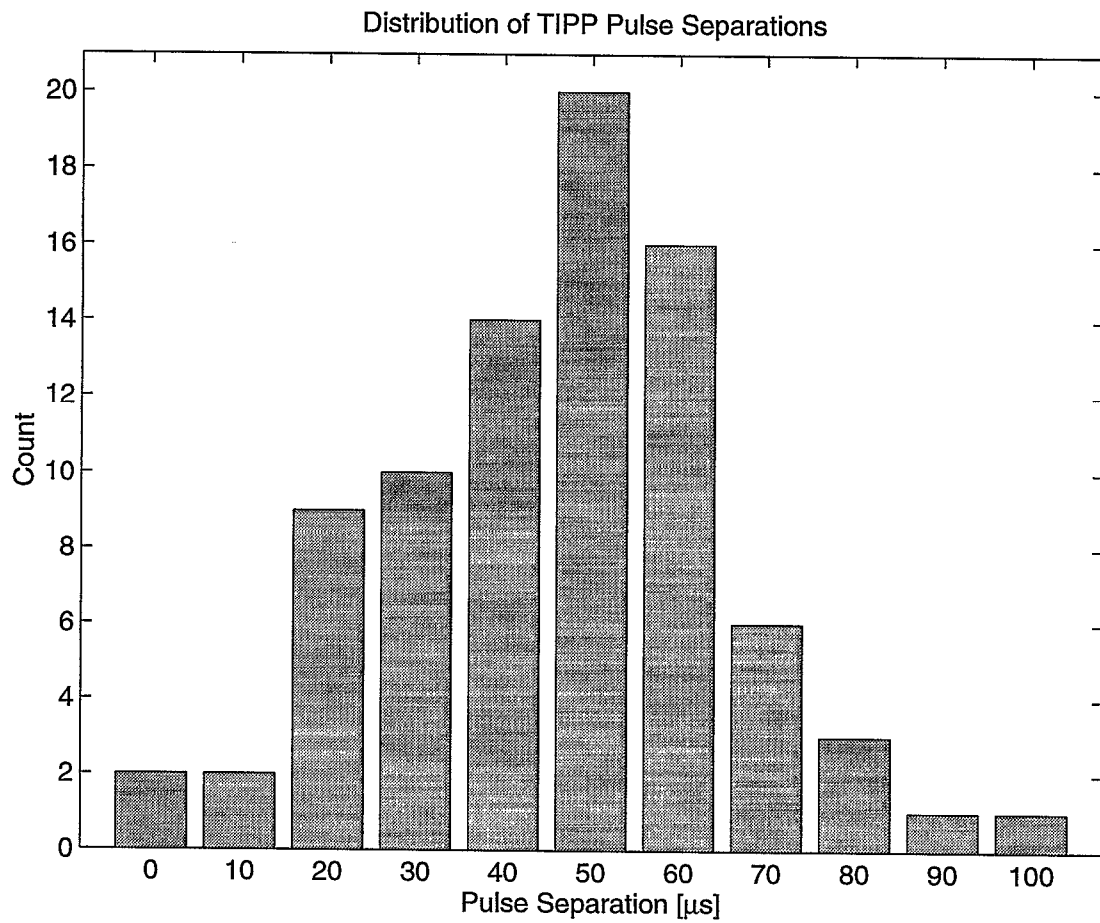


Figure 1.5: Distribution of pulse separations for 84 early TIPP events that were recorded by Blackbeard and analyzed by *Massey and Holden* [1995].

Equation 1.1 and Figure 1.4 are valid only for the case when $H \gg h$. A model presented by *Massey and Holden* [1995] showed that the distribution of pulse separations in Figure 1.5 is consistent with the typical TIPP source altitude being on the order of 15 km. This result is consistent with associations between TIPP events and thunderstorm activity [*Holden et al.*, 1995; *Smith*, 1995; *Smith and Holden*, 1996; *Zuelsdorf et al.*, 1997], since thunderstorms are tropospheric phenomena and the tropopause may extend as high as 20 km in the tropics. The fact that TIPPs are produced within a couple tens of kilometers of the surface of the earth means that the assumption that $H \gg h$ is always true for these events, since H is always approximately 800 km.

The one-source hypothesis also imposes requirements regarding the radiation pattern of the source and the reflectivity characteristics of the earth's surface at VHF frequencies. In order for the hypothesis to be valid, the following conditions must be met:

Firstly, the radiation pattern of the source must be broad in the vertical plane. This is so because the direct path and reflected path leave the source at quite different angles for events that occur with the satellite at a high elevation angle. For cases when the source lies close to the limb of the earth as viewed from Blackbeard, the angle between the direct and reflected paths is quite acute, but the broad distribution of time separations effectively rules out the possibility that this is always the case if TIPPs are produced in the troposphere.

Secondly, the typical surface reflectivity of the earth must be high (near unity) and reflections must be nearly specular in nature at VHF frequencies [*Massey and*

Holden, 1995; Massey et al., 1998]. These conditions must be met because TIPP second pulses contain, on average, almost as much energy as first pulses. In fact, of the first 84 low band TIPPs recorded, the second pulse actually had more energy than the first in 23 of the cases [*Massey and Holden, 1995*]. Thus if the one-source hypothesis is true, little energy can typically be lost at the earth reflection interface. It is also necessary to explain how it is possible for reflected pulses to have more energy than direct pulses when second pulses are subject to greater range loss (although only 0.8 dB for the worst-case scenario of a source at an altitude of 20 km and the satellite directly overhead at an altitude of 800 km) as well as reflection loss (although only 1.1 dB for poor soil conditions as concluded by *Massey et al. [1998]*). One possible explanation is that for some fraction of the events, the geometry of the reflection point may enhance the reflected signal. This could occur when mountains in the vicinity of the earth reflection point provided a greater reflecting area. A second explanation is that, depending on satellite/source geometry and the radiation pattern of the source, some fraction of the time the direct path to the satellite may be closer to a null in the source radiation pattern than the earth-reflected path.

Recent experimental results from *Massey et al. [1998]* suggest that the earth reflectivity requirements are met, even by the dry and sandy desert soil that was present where their experiment was carried out. Sandy soil is a worst case scenario, since its conductivity is low compared to other soils and much lower than sea water, which blankets most of the earth.

1.1.2 Two-Source Hypothesis

Under the two-source hypothesis the two TIPP emissions are assumed to be produced by two different, yet coupled, sources that are separated temporally and/or spatially. The lower panel of Figure 1.2 provides an illustration of this hypothesis. In order for the hypothesis to be consistent with Blackbeard data and an apparent lack of previous ground-based observations of powerful, paired pulses, the radiation pattern of the source must be directed upward. This is so for two reasons: 1. Strong pulse pairs have been absent from ground-based observations of high frequency emissions from lightning. If strong dual pulses are produced regularly by thunderstorms, then they would have most likely been observed from the ground, unless directed upward. 2. If TIPP second pulses are considered to be from a second source, then it must be questioned why reflections are not received. Either the source radiates primarily upward or the reflectivity of the earth is poor. Measurements by *Massey et al.* [1998] showed that the latter possibility is not true.

A theory describing a potential source for upward-propagating, paired radio flashes was published by *Roussel-Dupré and Gurevich* [1996]. In the theory, electrons with energies greater than a critical value are accelerated to high energies by thunderstorm electric fields that produce electrical forces greater than the frictional force of air. Impact ionization of the air by the energetic electrons leads to the production of energetic secondary electrons, whose energies also exceed the critical value. The net result is an avalanche in which the electron population grows exponentially. Collimation of the relativistic electrons by the electric field leads to

the formation of an electron beam. Signatures of this process would include optical, γ -ray, x-ray, and radio emissions. The radio emissions result from the acceleration and deceleration of the primary and secondary electron populations. Due to the relativistic nature of the process, the radio bursts are emitted primarily along an upward-directed cone. The angle of the cone from zenith depends on factors like the field strength, the number of avalanche lengths, and the air pressure, but is on the order of 15° . The runaway electron theory also has the potential for explaining observations of luminous flashes known as sprites and jets, which have been observed above thunderstorms [Sentman *et al.*, 1995; Wescott *et al.*, 1995]. It could also explain observations of x-ray pulses by instrumented balloons in thunderstorms [Eack *et al.*, 1996, a; Eack *et al.*, 1996, b] and observations of intense γ -ray flashes by the BATSE (Burst and Transient Signal Experiment) instrument on board the Compton Gamma Ray Observatory (CGRO) [Fishman *et al.*, 1994].

Observations and analyses presented in this paper will show that the one-source hypothesis is consistent with both Blackbeard and ground-based observations of radio signals from the source of TIPP events. The two-source hypothesis is not consistent with recent ground-based observations. The runaway electron theory by Roussel-Dupré and Gurevich [1996], however, still has the potential for explaining CIDs, the discharges that produce TIPP events (Robert Roussel-Dupré, private communication).

1.2 SUBIONOSPHERIC PULSE PAIRS (SIPPs)

Following the discovery of TIPP events in 1993 by Blackbeard, ground-based research campaigns were begun at Los Alamos National Laboratory to try to detect and characterize the events from *terra firma*. During the summer of 1994, a broadband data acquisition system was used to record signals over a frequency range from 3 to 30 MHz using a discone antenna. A discone antenna consists of a grounded cone, topped by a disc that serves as the receiving element. Data were digitized at 50 or 100 Msample/s after passing through a 30 MHz lowpass filter (at the 50 Msample/s sample rate, aliasing of the 25 to 30 MHz input signal to the 20 to 25 MHz frequency band occurred). The trigger for the digitizer was a specialized multiple-channel sub-band trigger that detected broadband transient signals against a background dominated by high-power CW signals. The instrumentation and subsequent observations were described by *Smith* [1995] and *Smith and Holden* [1996].

During the summer thunderstorm season, two classes of paired HF emissions were recorded and identified as candidates for the ground-recorded emissions from TIPP events. The two emission types were collectively dubbed subionospheric pulse pairs (SIPPs). One class of SIPPs was ionospherically dispersed, indicating propagation from over the horizon. The other class was undispersed, indicating line-of-sight propagation.

1.2.1 Dispersed Subionospheric Pulse Pairs

During the summer of 1994, seven dispersed SIPPs were recorded from over the horizon by the ground-based LANL broadband HF data acquisition system. The observations of obliquely propagated pulse pairs closely resembled Blackbeard observations of TIPP events in the following respects: the events occurred as pairs, were very powerful, and were temporally isolated from other transient RF signals. Two of the events were analyzed in detail and provided further evidence of an association between pulse pair events and thunderstorm activity [*Smith*, 1995; *Smith and Holden*, 1996].

An example of one of the events is shown in Figure 1.6. Two dispersed pulses are visible between 13 and 25 MHz against a background of multiple narrowband communication signals. The pulses were separated by 24 microseconds and demonstrated competing time-frequency effects that often characterize obliquely-propagated HF signals (a description of these effects was provided in Appendix B of *Smith* [1995]). The signal in Figure 1.6 was recorded within one minute of the signal in Figure 1.7, an emission with nearly identical dispersion characteristics, but which otherwise resembles HF radiation from a typical lightning streamer process. It was concluded that the similarity between the time-frequency properties of the events pictured in Figures 1.6 and 1.7 suggested that the two events originated in close proximity to each other. That the first emission was almost certainly from lightning indicates that the second emission, the pulse pair, originated in the vicinity of a thunderstorm.

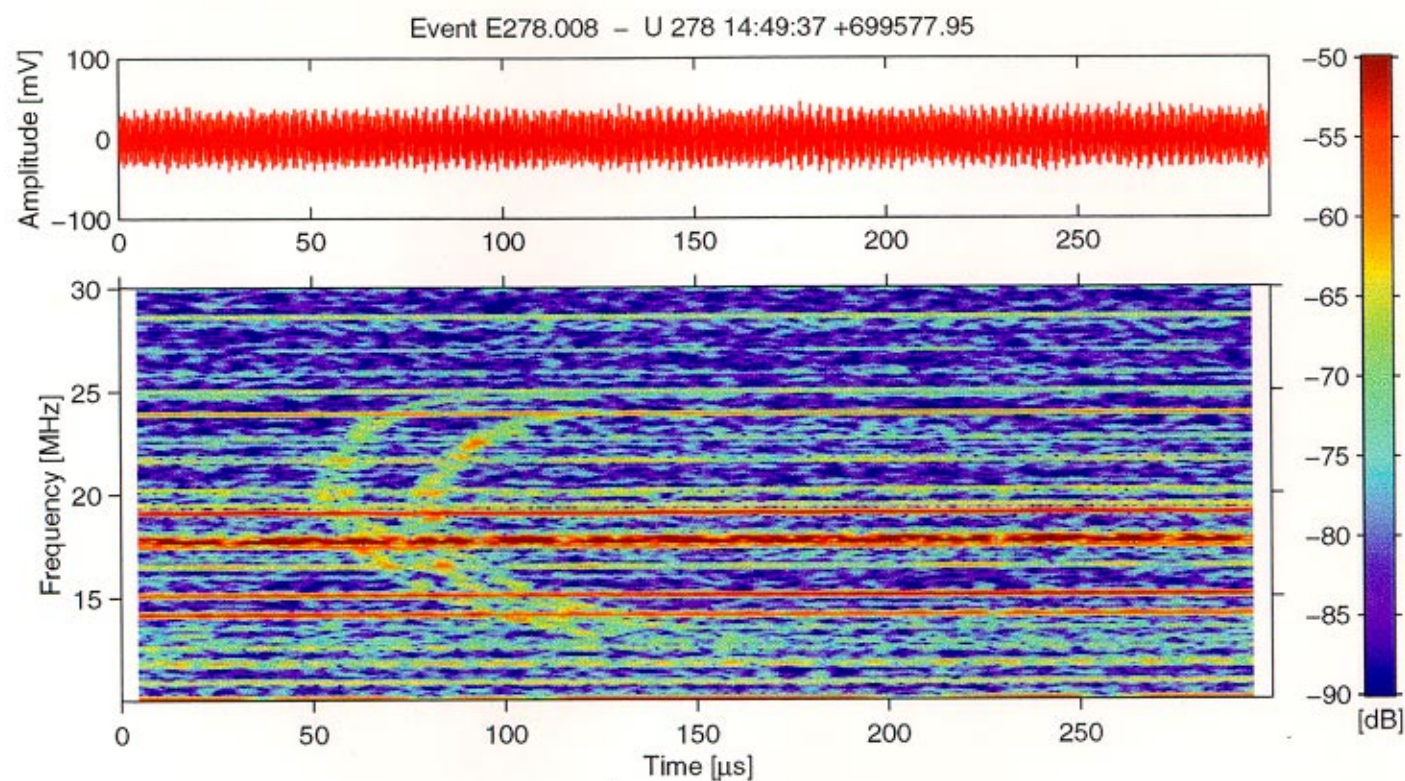


Figure 1.6: Time series and spectrogram for a subionospheric pulse pair (SIPP) that was recorded by the LANL ground-based broadband HF system during the summer of 1994. The dispersion of the two pulses indicate that they originated over the horizon and reflected from the ionosphere.

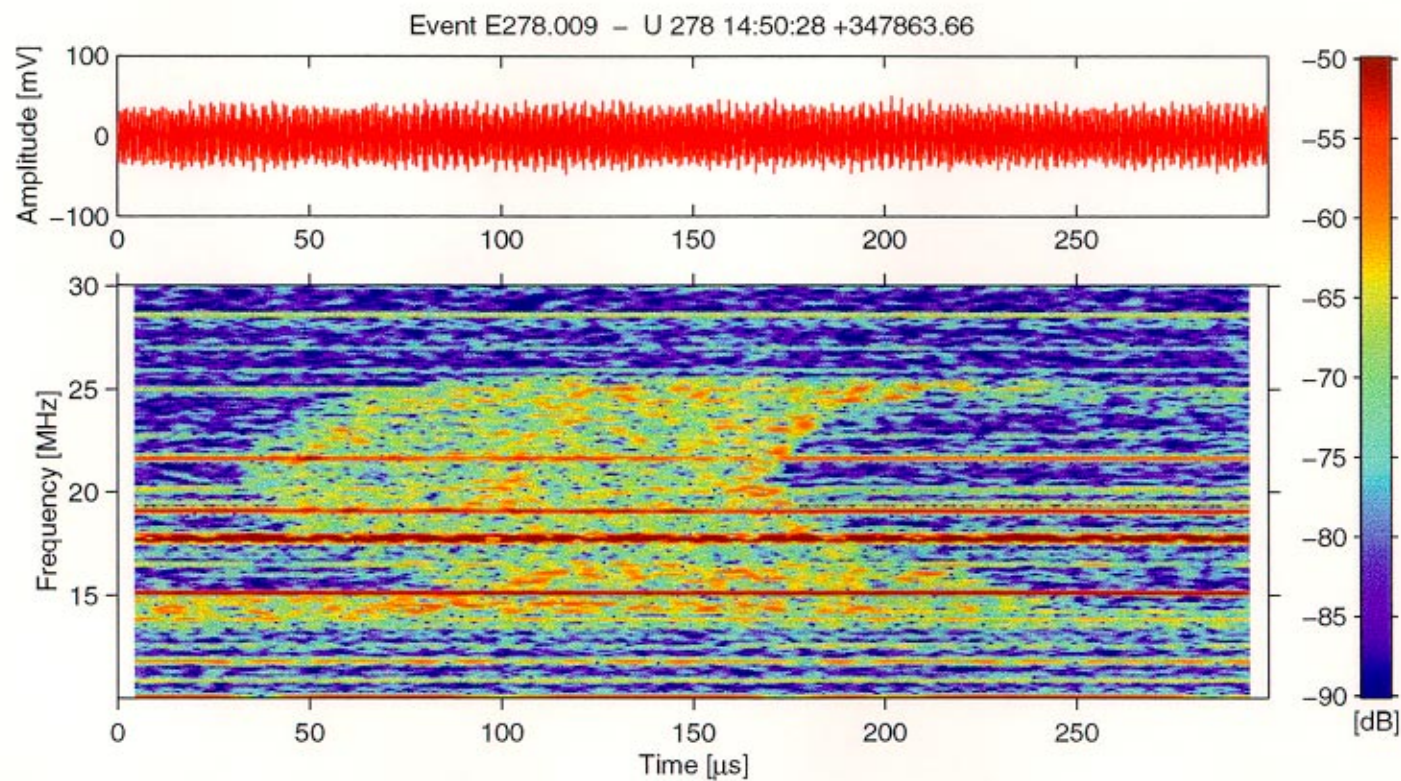


Figure 1.7: Time series and spectrogram for a dispersed burst of broadband radiation that was recorded by the LANL ground-based HF system during the summer of 1994. The source is believed to have been distant lightning.

1.2.2 Undispersed Subionospheric Pulse Pairs

Smith [1995] and *Smith and Holden* [1996] also described observations of undispersed SIPPs, pulse pairs for which all frequency components of the transient signals arrived at the receiver at the same time. An example of one of these events is shown in Figure 1.8. The time separation between the pulses was 22 μ s. The lack of dispersion indicates that the signals propagated from their source or sources to the receiver along line-of-sight propagation paths. The maximum line-of-sight reception range for HF signals is a function of the source and receiver heights. The LANL HF systems can make line-of-sight observations of thunderstorms from distances up to around 350 km.

It was stated by *Smith* [1995] and *Smith and Holden* [1996] that a lack of information about the locations of the sources of the undispersed pulse pairs made it impossible to compare their absolute signal strengths to those of TIPP events. This case was unlike that for the dispersed events because the fact that they were ionospherically dispersed guaranteed that the signals had distant origins. The authors stated that it was possible that the undispersed events actually had close origins and only appeared powerful as a result of their close proximity to the recording antenna. This author determined that this probably was the case, based on measurements made during the summer of 1997. A local anthropogenic RF emitter (a sodium lamp outside of the data acquisition lab) was identified as a source of intermittent nighttime radio pulse pairs. The discovery of the local source means that the observations of undispersed pulses pairs by *Smith* [1995] and *Smith and Holden* [1996] did not

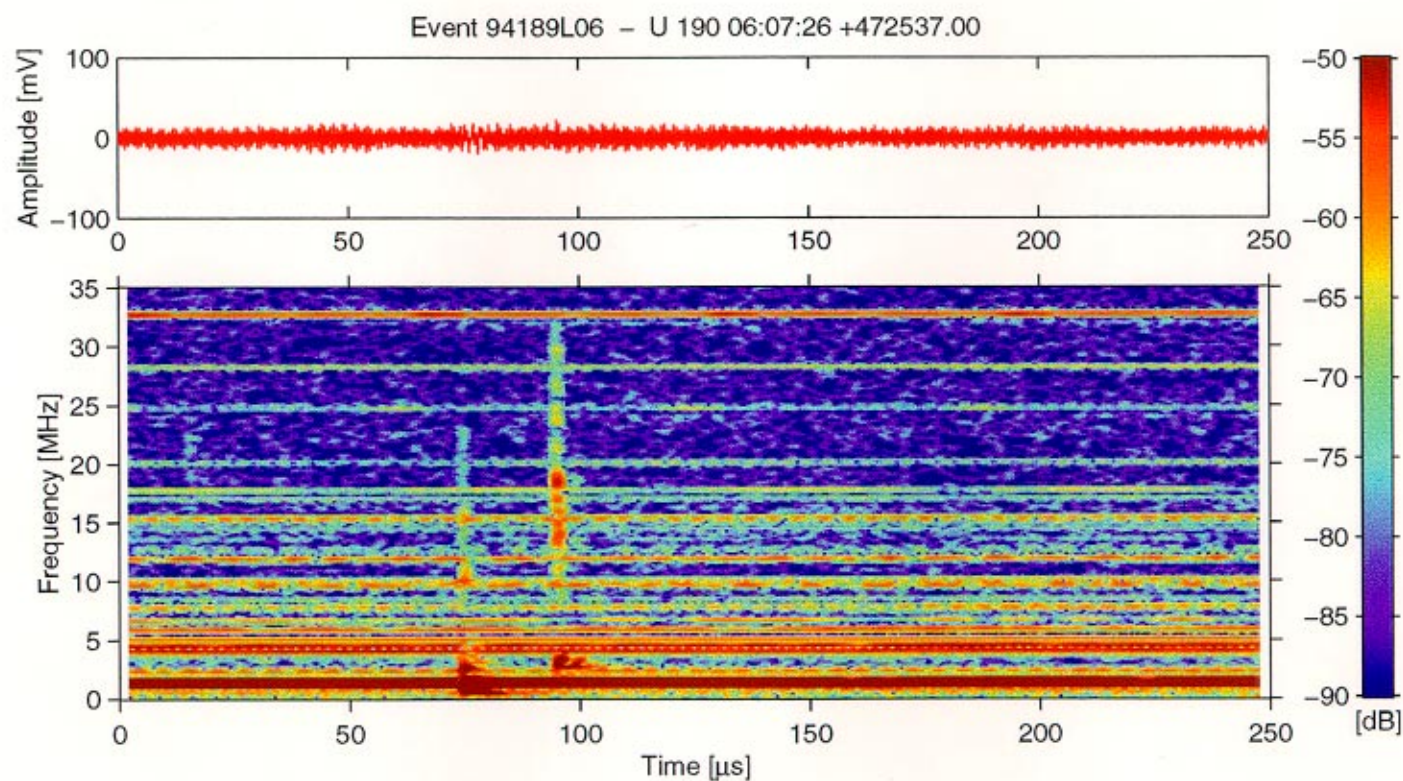


Figure 1.8: Time series and spectrogram for an undispersed subionospheric pulse pair that was recorded by the LANL ground-based HF system during the summer of 1994.

provide insight into TIPP phenomenology. The observations had provided support for the two-source hypothesis over the one-source hypothesis, since a ground-based receiver would receive the direct and earth-reflected pulses from a single source within nanoseconds of each other, not tens of microseconds.

1.3 NARROW POSITIVE BIPOLAR PULSES (NPBPs)

In the summer of 1996 thunderstorm observations were continued. Two somewhat independent research campaigns were begun at LANL. The ground-based HF system was expanded to three stations (separated by 6 to 13 km) so that events recorded by the three stations could be located using methods of differential time of arrival. The three stations were armed in conjunction with Blackbeard satellite passes to attempt to make simultaneous observations of TIPP events. The second campaign was conducted in cooperation with the New Mexico Institute of Mining and Technology (NMIMT). An array of three electric field change meters (separated by 30 to 230 km) was operated to detect, identify, and locate field change emissions from sprites.

During simultaneous operations of the two arrays in July of 1996, it was observed that occasional, narrow, large amplitude, bipolar electric field change pulses were recorded in conjunction with very powerful, broadband HF radiation. At the time, the HF systems were receiving trigger signals from one of the field change meters. The HF and field change pulses were almost always isolated from other transient radio

signals within their 1 ms and 5 ms respective records lengths. The signals were so distinct from other lightning emissions that, if not detected by multiple, widely-separated recording stations, the signals could easily have been mistaken as noise from a local transient source. The HF emissions from the source were exactly what was expected from the source of TIPP events under the one-source hypothesis: the RF bursts were singular, isolated, brief (lasting a few microseconds), broadband, and much more powerful than lightning signals emitted from the same storms. The sharp, isolated, bipolar field change pulses that were observed were similar to pulses previously observed by *Le Vine* [1980], *Willett et al.* [1989], and *Medelius et al.* [1991]. Following the first observations of these signals, simultaneous operations of the electric field change and HF arrays were begun.

Le Vine [1980] identified the “sources of the strongest RF radiation from lightning” as thunderstorm cloud processes consistently recorded in conjunction with distinct, short-duration (10-20 μ s overall), bipolar electric field change pulses. *Le Vine* [1980] used three narrowband receivers with center frequencies of 3, 139, and 295 MHz to trigger the acquisition of field change waveforms from an electric field change meter. When the trigger level of any of the RF receivers was set to a sufficiently high threshold during observations of thunderstorms, the corresponding electric field change waveforms were consistently isolated, short-duration, bipolar pulses. An example of a bipolar pulses from *Le Vine* [1980] is shown in Figure 1.9. Note that the polarity convention in the figure is opposite to that used throughout the remainder of this paper. Thus the pulse shown in Figure 1.9 is inverted compared to otherwise similar pulses presented here.

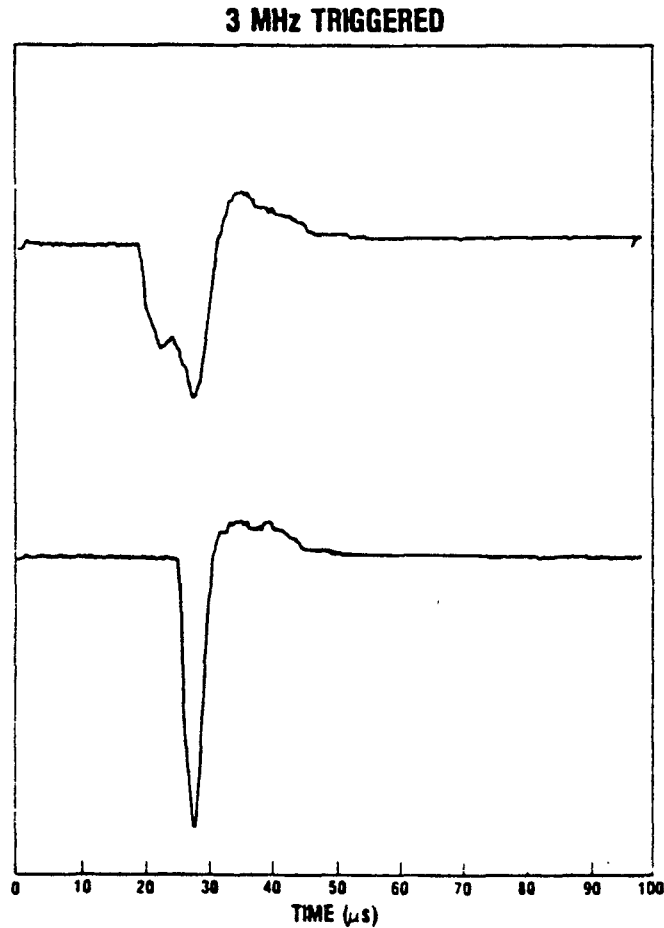


Fig. 2. Electric field changes triggered on RF radiation at 3 MHz (vertical polarization). The vertical scale is linear in V/m but uncalibrated. The direction of negative field change is down.

Figure 1.9: A narrow positive bipolar electric field change pulse recorded by LeVine [1980]. The field change meter was triggered by narrowband RF radiation centered at 3 MHz. The author used the opposite convention for electric field change polarity from that used throughout this dissertation. From D. M. Le Vine, *Journal of Geophysical Research*, 86, p. 4092, 1980, copyright by the American Geophysical Union.

Willett et al. [1989] made observations consistent with those of *Le Vine* [1980] using a large bandwidth (greater than 30 MHz) fast electric field change meter. The distinct, isolated, bipolar waveforms were emitted from thunderstorms that also produced normal lightning activity. An example of one of their waveforms is shown in Figure 1.10. The bipolar waveforms recorded by *Willett et al.* [1989] had a mean full width at half maximum (FWHM) of 2 μ s, overall durations of 20-30 μ s and peak amplitudes that were typically 0.72 times those from return strokes. *Willett et al.* [1989] dubbed the distinct field change waveforms narrow positive bipolar pulses (NPBPs). “Positive” refers to the initial polarity of the bipolar waveforms using the convention that a positive electric field change signal results from the deposition of negative charge overhead. *Willett et al.* [1989] also observed a few narrow negative bipolar pulses (NNBPs). The NNBPs were inverted in polarity, but otherwise similar to NPBPs in most respects. The authors concluded that “NPBPs are not usually associated with cloud-to-ground flashes, K changes in intracloud flashes, or other identified lightning processes.” They additionally concluded that “it is not obvious how any of the customary models of electromagnetic radiation from lightning could be credibly modified to produce such dE/dt signatures.”

Medelius et al. [1991] made wideband electric field and electric field change measurements of lightning at the Kennedy Space Center in 1989. They identified and characterized over 150 short-duration bipolar pulses with characteristics that closely matched the observations of *Le Vine* [1980] and *Willett et al.* [1989]. Pulses of both positive and negative polarity were observed with negative pulses being detected ten times more frequently than positive pulses. FWHM durations were on the order of a

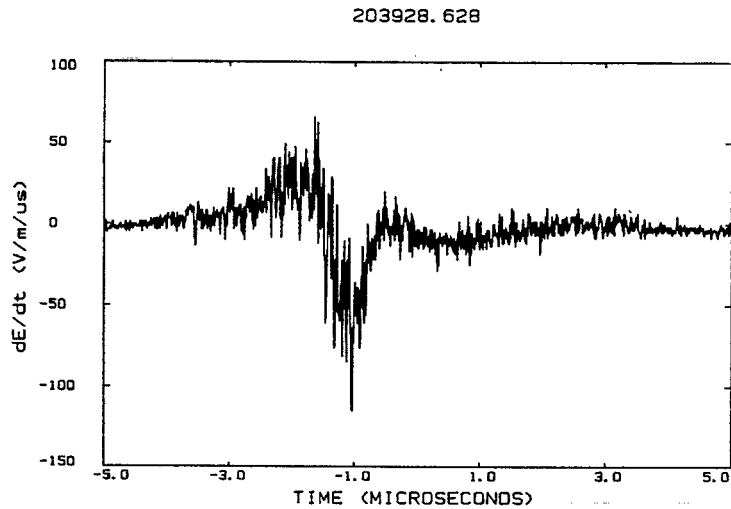
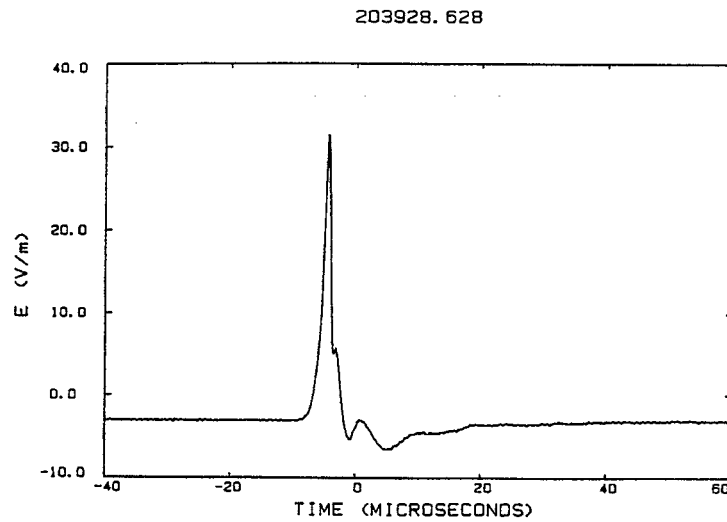


Fig. 2. Electric field (E) and field-derivative (dE/dt) waveforms for a typical narrow positive bipolar pulse (NPBP) from an isolated thunderstorm on July 24, 1985, centered 45 km away from our antennas. The "physics" sign convention is used here. Thus this pulse has the same polarity as those shown by *Le Vine* [1980], who used the opposite sign convention, and is opposite in polarity to a return stroke lowering negative charge (see Figure 3). Note the noisy appearance of dE/dt (shown on an expanded time scale) in comparison with E .

Figure 1.10: A narrow positive bipolar electric field change pulse recorded by Willett *et al.* [1989]. From J. C. Willett, J. C. Bailey, and E. P. Krider, *Journal of Geophysical Research*, 94, p. 16257, 1989, copyright by the American Geophysical Union.

few microseconds. Within a 30 event subset of the recorded bipolar pulses, two thirds were found to be isolated pulses that occurred with time separations of greater than one second from other lightning activity.

Electric field waveforms similar to those observed by *Le Vine* [1980], *Willett et al.* [1989], and *Medelius et al.* [1991] were described by *Weidman and Krider* [1979], *Cooray and Lundquist* [1985], and *Bils et al.* [1988]. The observations by these authors, however, were of pulses that lasted significantly longer and did not occur in isolation. The pulses were probably not from the same intracloud process that produces NPBPBs.

1.4 COMPACT INTRACLOUD DISCHARGES (CIDs)

NPBPBs, TIPPBs, and SIPPBs are produced by the same electrical discharges within thunderstorms. First evidence of this association was presented by *Shao et al.* [1996], *Smith et al.* [1996], and *Holden et al.* [1996]. *Smith et al.* [1997, b] presented calculations of the inferred physical properties of the discharge and provided evidence that the discharges were distinct from those that produce normal intracloud and cloud-to-ground thunderstorm electrical emissions. These unique discharges and the source regions that produce them are the primary topics of this dissertation. As a convenience, the sources of the distinct electrical emissions shall be referred to as CIDs (compact intracloud discharges) throughout the remainder of this paper.

Chapter 2 describes the instrumentation used to make measurements of thunderstorm electrical processes during the summer of 1996. The instrumentation includes the three-station electric field change array, the three-station broadband HF array, and the Blackbeard broadband satellite receiver. Chapter 3 provides a description of the techniques used to locate emission sources using methods of time of arrival. Reflections of signals from the ionosphere and earth provided a powerful means of accurately determining source altitudes. Chapter 4 describes observations of three nighttime convective airmass thunderstorms that produced CIDs. The storms occurred in the southwestern US during July and August of 1996. Chapter 5 describes observations of tropical cyclone Fausto, which produced CIDs on two different nights in September of 1996. Chapter 6 summarizes observations of the recorded emissions in detail and provides an overview of their source regions. In Chapter 7, the phenomenology of CID emissions is used to determine fundamental characteristics of the source region and the discharge itself. Chapter 8 provides a final summary of the conclusions. For the reader's convenience, a glossary of terms and acronyms has been provided following Chapter 8.

CHAPTER 2

INSTRUMENTATION

Two arrays of ground-based sensors in northern New Mexico were utilized to observe and locate radio emissions from thunderstorms during the summer of 1996. Data and timing information from the Blackbeard instrument on the ALEXIS satellite were also used to locate and characterize thunderstorm emissions.

The first array consisted of three independent electric field change meters equipped with digital data acquisition and GPS (Global Positioning System) timing systems. The stations were separated by distances ranging from 30 to 230 km. The locations of emission sources were determined from differential times of arrival (DTOAs) of signals recorded by the stations. Reflections of field change signals from the ionosphere and ground were often recorded by the stations in addition to the groundwave signals. The reflections provided vertical time of arrival (TOA) baselines for the determination of accurate three-dimensional (3-D) source locations.

The second array consisted of three broadband HF data acquisition systems also equipped with digital data acquisition and GPS timing. The stations were separated by distances ranging from 6 to 13 km. Unlike the field change systems, the HF systems were not triggered independently. A VHF communication system transmitted trigger signals from the primary station to the two remote stations each time the

primary station received a trigger. The communication system ensured that the three stations acquired data approximately coincidentally. HF times of arrival were also used in the determination of 3-D source locations.

Figure 2.1 shows the locations of the three fast electric field change systems (FC1, FC2, and FC3) and three broadband HF systems (HF1, HF2, and HF3). The primary HF system (HF1) was co-located with the Los Alamos electric field change system (FC1) at LANL. The Albuquerque NEXRAD weather surveillance radar (ABX), from which radar reflectivity data were acquired, is also shown, along with the locations of three thunderstorms (1, 2, and 3) from which the ground-based observations described in Chapter 4 were made.

2.1 ELECTRIC FIELD CHANGE INSTRUMENTATION

The locations of the three electric field change systems (FC1, FC2, and FC3) are represented by circles in Figure 2.1. FC1 was operated by LANL from Los Alamos, NM. The field change meter was co-located with the primary broadband HF station, which is described in the following section. FC2 was operated by the New Mexico Institute of Mining and Technology (NMIMT) from the Langmuir Laboratory for Atmospheric Research, located 27 km west of Socorro, NM. FC3 was also operated by NMIMT, but from a residence located 6 km north-northeast of Socorro. The distances between the stations were (FC1-FC2) 224 km, (FC2-FC3) 30 km, and (FC3-FC1) 206 km.

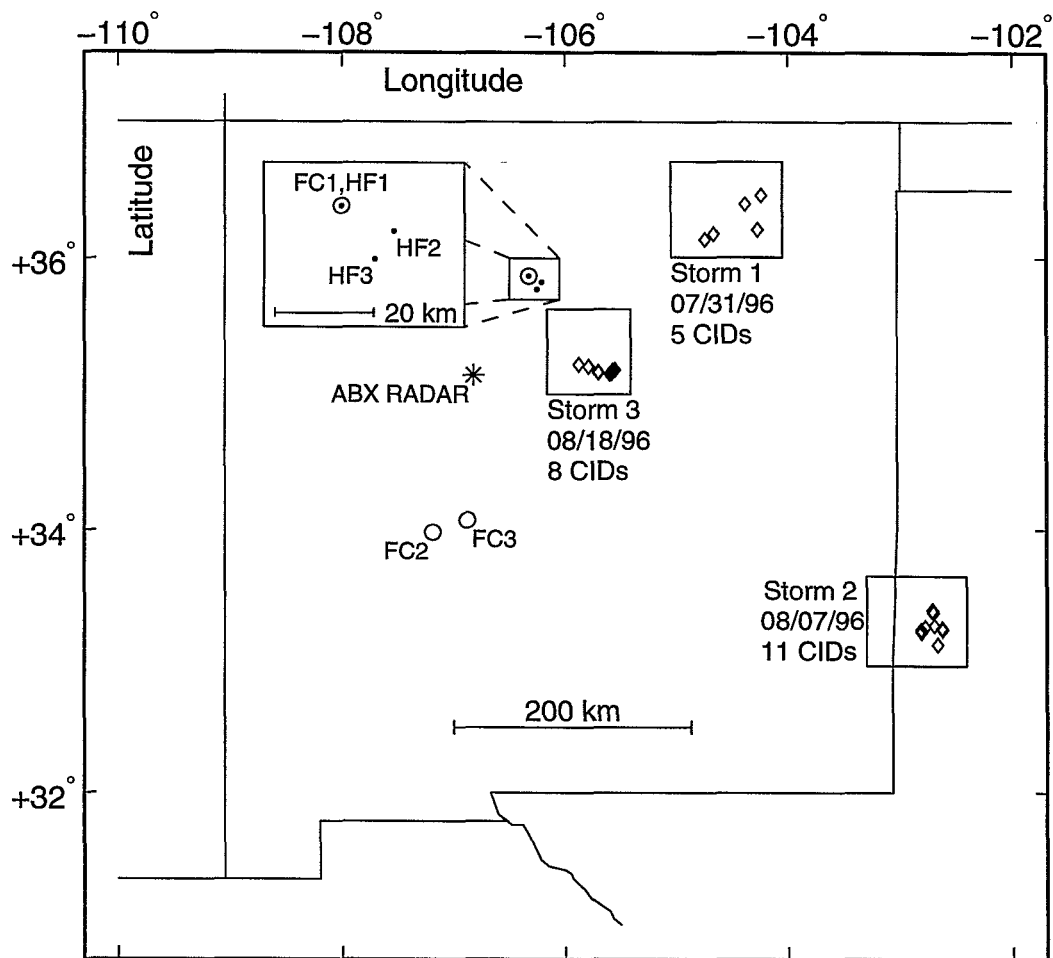


Figure 2.1: Plan view locations of the electric field change stations (FC1, FC2, and FC3), the broadband HF stations (HF1, HF2, and HF3), and the Albuquerque NEXRAD radar (ABX). Also shown are the locations of the three thunderstorms (1, 2, and 3) that were studied during the summer of 1996. CID locations in the storms are represented by diamonds.